

# Trapping of two-component matter-wave solitons by mismatched optical lattices

Z. Shi<sup>1</sup>, K.J.H. Law<sup>1</sup>, P.G. Kevrekidis<sup>1</sup>, and B.A. Malomed<sup>2</sup>

<sup>1</sup> *Department of Mathematics and Statistics, University of Massachusetts, Amherst MA 01003-4515, USA*

<sup>2</sup> *Department of Physical Electronics, School of Electrical Engineering, Faculty of Engineering, Tel Aviv University, Tel Aviv 69978, Israel*

We consider a one-dimensional model of a two-component Bose-Einstein condensate in the presence of periodic external potentials of opposite signs, acting on the two species. The interaction between the species is attractive, while intra-species interactions may be attractive too [the system of the bright-bright (BB) type], or of opposite signs in the two components [the *gap-bright* (GB) model]. We identify the existence and stability domains for soliton complexes of the BB and GB types. The evolution of unstable solitons leads to the establishment of oscillatory states. The increase of the strength of the nonlinear attraction between the species results in *symbiotic stabilization* of the complexes, despite the fact that one component is centered around a local maximum of the respective periodic potential.

## I. INTRODUCTION

Optical lattices (OLs) offer a powerful and ubiquitous tool for the creation and control of various patterns in Bose-Einstein condensates (BECs). OLs are induced by the interference of counterpropagating coherent laser beams illuminating the condensate and creating an effective periodic potential for atoms [1]. A well-established fact is that OLs support *gap solitons* in BECs with repulsive interactions between atoms. Effectively one-dimensional (1D) gap solitons were predicted [2] and then created experimentally in BECs filling a “cigar-shaped” trap, which acted in the combination with an OL induced in the axial direction. In self-attractive media, periodic potentials allow one to capture a soliton at a prescribed position, and also give rise to stable multi-soliton complexes. In fact, the model of a medium with the cubic self-attractive nonlinearity and effective periodic potential applies not only to BEC but also to optics, where it predicts spatial solitons in a planar waveguide with a transverse modulation of the local refractive index. Actually, the model was first put forward in the latter context, and fundamental solitons, as well as their bound states, were found in it [4]. Later, the same model was introduced in the context of the mean-field dynamics in BECs [5].

Another topic of great interest to BECs is the study of binary condensates, which are most typically generated as mixtures of two different hyperfine atomic states, with opposite values of the  $z$ -projection of the atomic spin [6]. The interactions between atoms belonging to the same [7] and different [8] hyperfine species can be controlled (including a possibility to reverse the sign of the interaction) by means of the Feshbach resonance. In particular, one may consider a binary condensate that features intra-species repulsive interactions combined with attraction between the species. It was predicted that the latter setting may give rise to *symbiotic* soliton complexes [9], which are held together by the attraction overcoming the intrinsic repulsion.

Specific types of BEC solitons have also been predicted in settings assuming a binary condensate trapped in OLs. In particular, the interplay of the repulsion between the two species, if combined with the dynamical effect induced by the lattice (an effective negative mass of collective excitations) may give rise to 1D and 2D *symbiotic gap solitons* [10, 11], even in the case when the intra-species interaction is switched off. The addition of the intra-species repulsion helps to expand the stability region of the symbiotic gap solitons [10], while the interplay of the OL effects, intra-species attraction, and repulsion between the two species gives rise to other new types of solitons complexes, such as *semi-gap* ones, with one of the components belonging to the semi-infinite gap in the OL-induced linear spectrum, while the other component sits in a finite bandgap [11]. The case of the attraction between two self-repulsive species was recently considered in Ref. [12], where it was demonstrated that the attraction leads to a counter-intuitive result, *viz.*, *splitting* between gap solitons formed in each species. This effect is explained by a negative effective mass of gap solitons, which is one of their principal characteristic features [2].

In fact, the OL potentials acting on two species in a binary BEC need not be identical. For example, if the actual source of the potential is not an OL, but rather a periodically nonuniform distribution of a magnetic field (acting in direction  $z$  and modulated along  $x$ ), which couples to the atomic spin (while the basic trap is optical), then the effective potential will, obviously, have opposite signs for the atomic states with opposite values of the  $z$ -component of the spin. An issue of straightforward interest is then to consider two-component soliton complexes supported by pairs of *mismatched lattices*. In particular, effects of the mismatch on two-component 1D and 2D gap solitons with *linear* coupling between the components (which corresponds to BEC loaded into two parallel tunnel-coupled traps) were studied in Refs. [13]. It was found that the mismatch affects the *spontaneous symmetry breaking* (SSB) bifurcation that accounts for a transition from symmetric or antisymmetric solitons to asymmetric

ones: the symmetric/antisymmetric states are replaced by their *quasi*-symmetric/antisymmetric counterparts, but the bifurcation still occurs. An exception is the limit case when the phase shift between the lattices is  $\pi$  (i.e., the two OL potentials are mutually opposite) – then, the bifurcation is replaced by a *pseudo-bifurcation*, in which branches of quasi-symmetric/antisymmetric and asymmetric solutions asymptotically approach each other, but never meet [13]. Effects of the mismatch between two gratings on the SSB bifurcations of optical gap solitons were also studied in the model of two linearly coupled parallel fiber Bragg gratings, which is an optical counterpart of the OL pair in the BEC model [14] (“light bullets” in an array of Bragg gratings with alternating signs were considered in Ref. [15]).

The objective of the present work is to study 1D two-component solitons with the ordinary nonlinear *attraction* between the species, assuming that they are subject to the action of periodic potentials *with opposite signs*. The model corresponds, in particular, to the above-mentioned mixture of two atomic states with opposite values of the spin, that couples to a periodically modulated distribution of the magnetic field. Issues of straightforward interest are the existence and stability of two-component solitons. The stability problem is quite nontrivial in this setting, as, on the one hand, the soliton complex tends to be unstable because one of its constituent components is placed around a local maximum of the respective potential, but, on the other hand, the complex may be stabilized by the attraction between the components. We consider two varieties of the model, with either intrinsic attraction in both components [the respective soliton complexes are categorized as *bright-bright* (BB) ones], or opposite signs of the intra-species interaction [which corresponds to *gap-bright* (GB) complexes].

It is necessary to mention that various solutions (chiefly of the solitary wave type) in models of two-component BEC mixtures trapped in OLs, with attractive inter- and intra-species interactions, were considered in several works [16, 17]. In most cases, the periodic potentials acting on both species were essentially identical (in-phase) [16], although an example with the phase shift of  $\pi/2$  between the two potentials was considered too [17] (the latter work was chiefly dealing with soliton complexes of the dark-bright type). However, the settings studied in the present work were not considered before, to the best of our knowledge.

The rest of the paper is organized as follows. We formulate the model in Sec. II, and summarize results for both types of the soliton complexes, of the BB and GB types, in Sec. III. Stability regions in a relevant parameter space are identified through the numerical computation of eigenvalues for small perturbations. The evolution of unstable solitons is explored by means of systematic direct simulations. The paper is concluded by Sec. IV.

## II. THE MODEL

The starting point is the system of coupled 1D Gross-Pitaevskii equations for the mean-field wave functions of the two BEC species,  $U_1$  and  $U_2$  [18]. In the usual scaled form, the system is

$$i\frac{\partial U_j}{\partial t} = -\frac{1}{2}\frac{\partial^2 U_j}{\partial x^2} + \sum_{k=1}^2 g_{jk}|U_k|^2 U_j + V_j(x)U_j, \quad (1)$$

with  $j, k = 1, 2$ , where  $g_{jk} \equiv 4a_{jk}\sqrt{m\Omega/\hbar}$  are effective interaction coefficients ( $a_{jk}$  are scattering lengths of the respective interatomic interactions,  $m$  the atomic mass, common for both species, and  $\Omega$  the transverse trapping frequency), and  $V_j(x)$  are the normalized OL potentials, which are different for the two components. In accordance with the scaling, the numbers of atoms in the two species (their norms) are  $N_j = \int_{-\infty}^{+\infty} |U_j(x)|^2 dx$ . As usual, we seek for stationary solutions to Eqs. (1) with chemical potentials  $\mu_j$  as  $U_j(x, t) = \exp(-i\mu_j t)u_j(x)$ , where the real functions  $u_j$  obey the equations

$$\mu_j u_j = -\frac{1}{2}\frac{d^2 u_j}{dx^2} + \sum_{k=1}^2 g_{jk}u_k^2 u_j + V_j(x)u_j. \quad (2)$$

Localized solutions to Eqs. (2) were obtained through fixed-point (Newton-Raphson) iterations, using initial guesses for both components in the form of sech functions. As indicated in the introduction, the situations that we focus on here are of the BB and GB types, i.e., ones with self-attraction in both components ( $g_{11}, g_{22} < 0$ ), or opposite signs of the self-interaction ( $g_{11} > 0$  and  $g_{22} < 0$ ), respectively.

Once the numerical solution to Eq. (2) was found, its stability was investigated against infinitesimal perturbations  $\{a_j, b_j\}$  with growth rate  $\lambda \equiv \lambda_{\text{real}} + i\lambda_{\text{imag}}$ , taking the perturbed solution as

$$U_j(x, t) = \exp(-i\mu_j t) [u_j + a_j(x)\exp(\lambda t) + b_j^*(x)\exp(\lambda^* t)], \quad (3)$$

and solving the eigenvalue problem generated by the substitution of this expression in Eqs. (1) and linearization. Sets of unstable complex eigenvalues of the resulting Hamiltonian eigenvalue problem arise in quartets, i.e., if  $\lambda$  is

an eigenvalue, then so are  $-\lambda$ ,  $\lambda^*$  and  $-\lambda^*$ , hence the existence of any  $\lambda_{\text{real}} \neq 0$  implies instability (real eigenvalues come in pairs,  $\pm\lambda$ , which also gives rise to instability). The eigenvalue problem was solved by using a finite-difference discretization [in the same way as it was used to solve the stationary version of Eq. (1)]. The latter method reduces the problem to finding matrix eigenvalues, which can be done by means of standard numerical linear algebra packages.

If a configuration is found to be unstable, an outcome of the instability development was concluded from direct simulations. To that effect, we used an integrator implemented on the basis of the fourth-order Runge-Kutta method, with initial conditions taken as per exact numerically found stationary states, with the addition of weak perturbations seeding the instability growth.

### III. RESULTS: TWO-COMPONENT SOLITONS AND THEIR STABILITY

#### A. Bright-bright solitons

The OL potentials acting on the two species are assumed to be of the form

$$V_1(x) = V_{01} \sin^2(kx), \quad V_2(x) = V_{02} \cos^2(kx), \quad (4)$$

which obviously corresponds to the phase shift of  $\pi$  between the sublattices. Figures 1-4 provide a systematic presentation of the results, with a typical value of the wavenumber,  $k = \pi/5$ . First, profiles of a pair of two-component solitons of the BB type, one unstable (through a pair of real eigenvalues), and the other one stable, are displayed in Fig. 1. In either case, both components of the soliton are originally centered at  $x = 0$ . In accordance with this, the component  $U_1$ , which is centered around its local potential minimum [see Eq. (4)] is a stable one, while  $U_2$ , whose original location coincides with a local *maximum* of the respective potential,  $V_2(x)$ , may be unstable.

The evolution of the unstable soliton shown in Fig. 2 (the one pertaining to  $g_{12} = -0.04$ ) was examined by means of direct simulations, as shown in Fig. 2. It is seen that the stable component ( $U_1$ , in this case), remains centered around the minimum of the corresponding potential well,  $x = 0$ , while the unstable component ( $U_2$ ) is displaced by the instability and ends up in an oscillatory state around a nearby minimum of its respective potential,  $x = \pi/(2k) \equiv 5/2$ . This is a typical scenario of the instability development observed in the present setting.

Results of a systematic analysis of the existence and stability of the soliton family are presented in Figs. 3 and 4. Figure 3 shows a continuation of the family in  $g_{12}$ , the cross-coupling interaction strength. At  $g_{12} = 0$ , the configuration is obviously unstable, due to the fact that one of the solitary waves ( $U_2$ ) is sitting on top of a potential maximum (see, e.g., Ref. [19] and references therein for a rigorous investigation of the instability). As the interaction between the two components gets enhanced, the stable first component creates an effective attractive potential for the second component, that eventually [in Fig. 3, this happens at  $g_{12} < -0.19$ ] overcomes the repulsive effect of the local potential  $V_2$ , and thus makes the configuration stable. Due to this mechanism, one may speak about *symbiotically stabilized* solitary waves. As the continuation progresses towards more negative values of  $g_{12}$ , the second component eventually disappears, and the resulting single-component bright soliton is no longer affected by  $g_{12}$ .

Full results are summarized in the two-parameter soliton stability diagram displayed of Fig. 4, with the grayscale indicating the magnitude of the unstable eigenvalue. The stability border between the linearly stable and linearly unstable regions is given by the curved (red in the online version) line.

#### B. Solitons of the gap-bright type

Typical examples of stable and unstable stationary states of the GB type are shown in Fig. 5. In this setting, the potentials are again taken as in Eq. (4). The stable component,  $U_1$ , is always of the gap type (i.e., with the repulsive intrinsic interaction,  $g_{11} > 0$ ), while the self-attractive (“bright”) component,  $U_2$ , with  $g_{22} < 0$ , may be unstable.

The examples displayed in Fig. 5 correspond to  $\mu_1 = 0.6$ , which actually falls in the middle of the first bandgap in the OL-induced linear spectrum of the first component. For this reason, the gap-type component ( $u_1$ ) does not feature conspicuous tails [10, 20]. Taking a larger value of the chemical potential, for instance,  $\mu_2 = 0.88$ , which is chosen closer to the edge of the bandgap, we can generate the gap-components of the soliton with more salient tails, see Fig. 6.

Simulations of the evolution of unstable complexes of the GB type, as shown in Fig. 7, reveal an essential difference from the instability-development pattern that was observed in the previous case (for the two-component solitons of the BB type). In that case, independently of the specific value of  $g_{12}$ , the stable component (which was also  $U_1$ ) remained centered around  $x = 0$ , while the unstable one,  $U_2$ , oscillated around either of the two nearby minima of its respective potential, see Fig. 2. On the other hand, component  $U_2$  in the case of unstable GB solitons *splits* into two

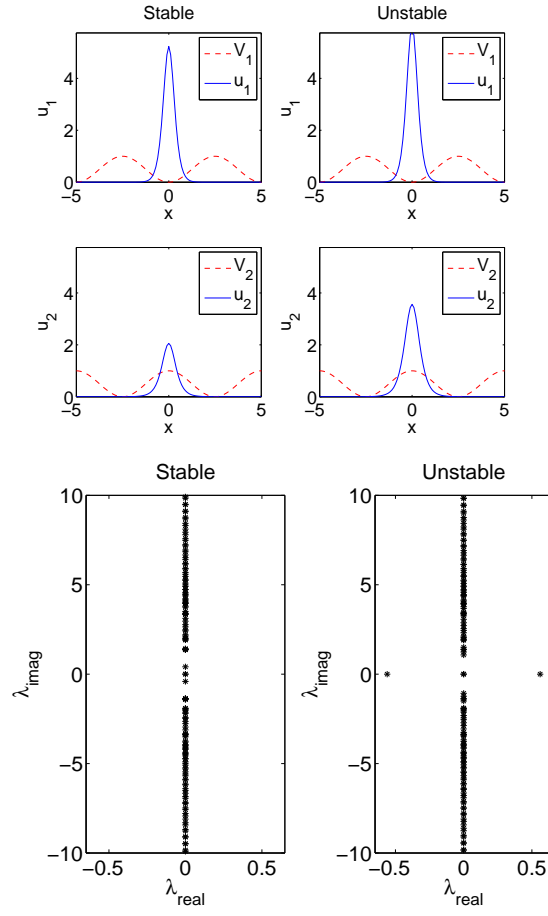


FIG. 1: (Color online) Profiles of both components of stable and unstable solitons of the bright-bright type. The corresponding parameters in Eqs. (2) and (4) are  $V_{01} = V_{02} = 1$ ,  $\mu_1 = -3$ ,  $\mu_2 = -1$ ,  $g_{11} = -1$ ,  $g_{22} = -1$ , and  $(g_{12})_{\text{st}} = -0.4$  or  $(g_{12})_{\text{unst}} = -0.04$ , for the stable and unstable solitons, respectively. The solid and dashed lines show the profiles of the components and of the periodic potential, respectively. The bottom panel shows the respective spectral planes of the stability eigenvalues,  $\lambda = \lambda_{\text{real}} + i\lambda_{\text{imag}}$ , which identifies the left and right solitons as stable and unstable ones, respectively.

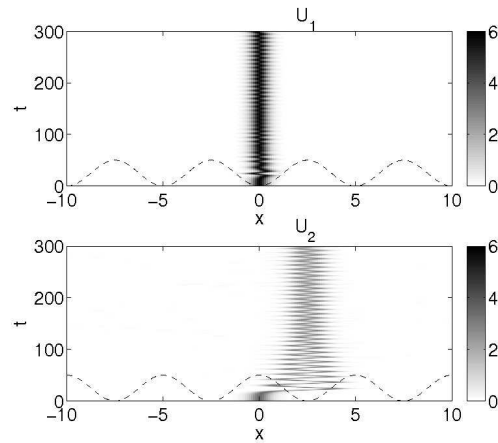


FIG. 2: (Color online) The dynamics of both components of an unstable soliton complex of the bright-bright type is shown by means of density space-time contour plots. The parameter setting is the same as in the unstable case of Fig. 1.

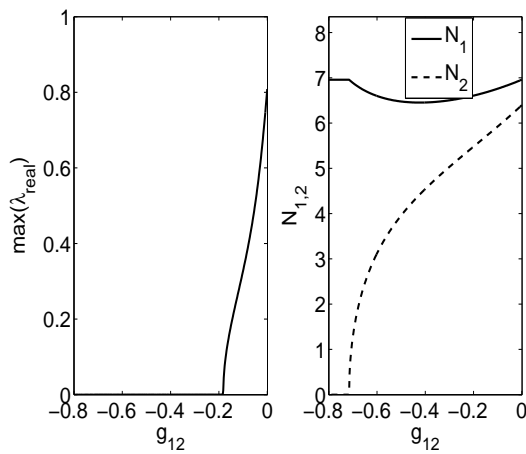
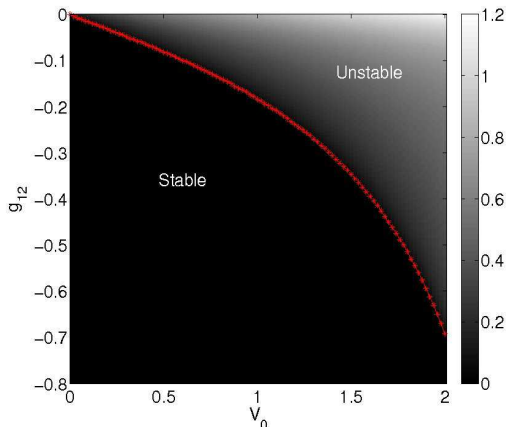


FIG. 3: (Color online) The change of the stability of the bright-bright soliton (shown through the largest instability growth rate), and the variation of the norms of both of it's components, as  $g_{12}$  decreases from 0 to  $-1$ . Other parameters are  $V_{01} = V_{02} = 1$ ,  $\mu_1 = -3$ ,  $\mu_2 = -1$ ,  $g_{11} = g_{22} = -1$ .

FIG. 4: (Color online) The stability diagram for the soliton complexes of the bright-bright type in the plane of  $V_{01} = V_{02} \equiv V_0$  and  $g_{12}$  (the stability is identified as per the maximum value of growth rate  $\lambda_{\text{real}}$  whose contour plot is shown). The other parameters are  $\mu_1 = -3$ ,  $\mu_2 = -1$ ,  $g_{11} = g_{22} = -1$ . The black color means that the soliton complex is stable ( $\lambda_{\text{real}} \equiv 0$ ); the lighter the color, the more unstable the soliton is. The curved line indicates the stability border, as found from the numerical data.



*unequal* parts, if the interaction between the two components is weak (see, e.g., an example for  $g_{12} = -0.15$  in the top two rows of Fig. 7). The two splinters end up oscillating around different nearby potential minima,  $x = \pm 5/2$ . As  $|g_{12}|$  rises to intermediate values, such as  $g_{12} = -1$ , the unstable component  $U_2$  of the GB soliton ceases to feature splitting, but rather oscillates around one of the minima, while the first (stable) component,  $U_1$ , is found to oscillate between its original position,  $x = 0$ , and an adjacent potential minimum,  $x = -2\pi/(2k) \equiv -5$  (in fact,  $U_1$  oscillates around the average position of component  $U_2$ ). These scenarios of the instability development are displayed in the third and fourth rows of Fig. 7). As the interaction between the components becomes still stronger – for instance, at  $g_{12} = -1.65$  – both components feature approximately *synchronous* oscillations (i.e., the soliton complex keeps its integrity, due to the strong attraction between its constituents) in the range of  $-2.5 < x < 0$ , that is, between the minimum of potential  $V_1(x)$ /maximum of  $V_2(x)$  and the adjacent maximum of  $V_1(x)$ /minimum of  $V_2(x)$ .

Performing the continuation in the interaction-strength parameter,  $g_{12}$ , we have generated characteristics of the GB-soliton family, a typical example of which is displayed in Fig. 8, cf. Fig. 3 for complexes of the BB type. Further, collecting the results for different values of  $V_{02}$  [while  $V_{01}$  is fixed, see Eq. (4)], we have produced the stability diagram for the GB solitons, as shown in Fig. 9, cf. its counterpart for the solitons of the BB type in Fig. 4. It is worthy to note that the critical value of  $g_{12}$  at the stability border decreases almost linearly as  $V_{02}$  increases.

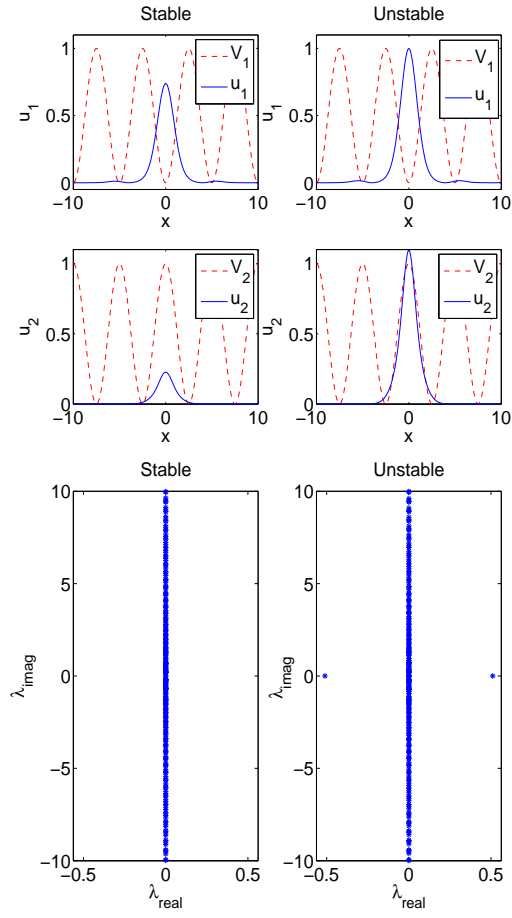


FIG. 5: (Color online) Profiles of both components of gap-bright soliton complexes in stable and unstable states. The parameters are:  $V_{01} = V_{02} = 1$ ,  $\mu_1 = 0.6$ ,  $\mu_2 = -0.3$ ,  $g_{11} = 1$ ,  $g_{22} = -1$ , and  $(g_{12})_{\text{st}} = -2.0$ ,  $(g_{12})_{\text{unst}} = -0.675$ , for the stable and unstable solitons, respectively.

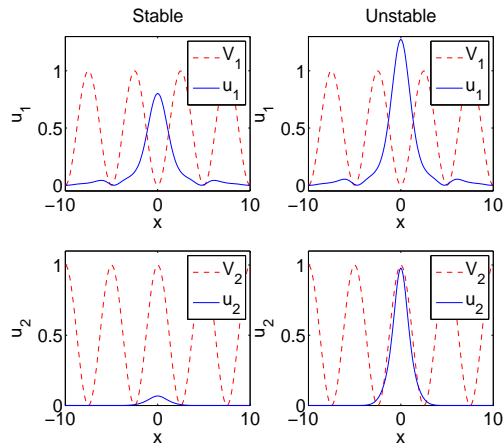


FIG. 6: (Color online) The same as in Fig. 5, except for  $\mu_1 = 0.88$ ,  $\mu_2 = -0.4$ , and  $(g_{12})_{\text{st}} = -2.00$ ,  $(g_{12})_{\text{unst}} = -0.675$ .

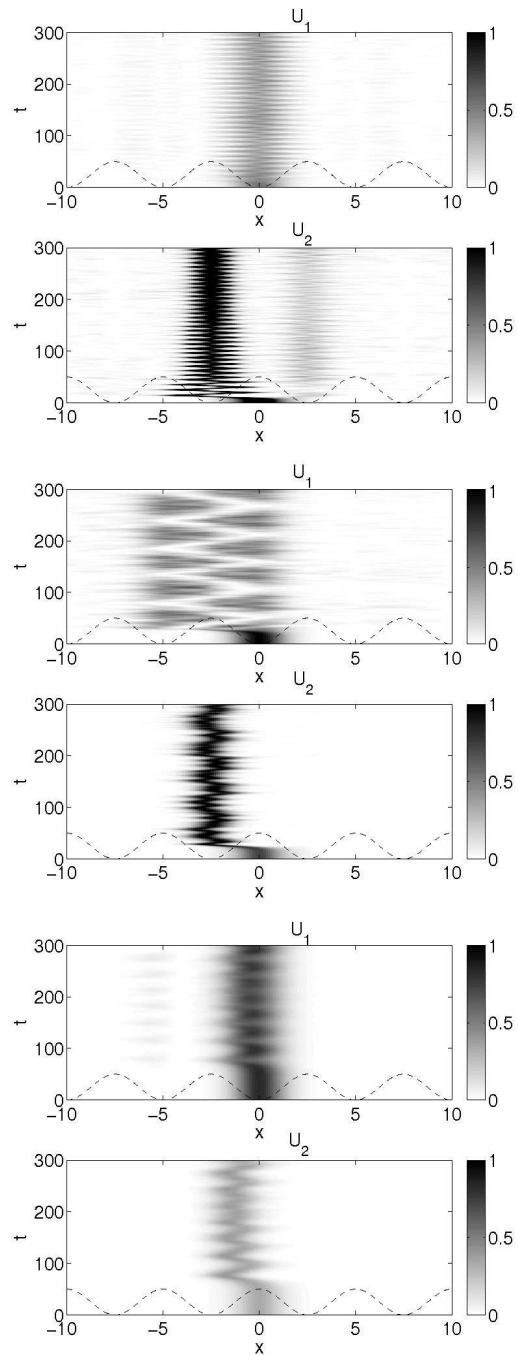


FIG. 7: (Color online) The evolution of an unstable soliton complex of the gap-bright type. Parameters are the same as in the former pictures displaying the gap-bright complexes, except that  $g_{12} = -0.15$ ,  $g_{12} = -1.00$ , and  $g_{12} = -1.65$ , in the top two rows, third and fourth rows, and bottom two rows, respectively.

#### IV. CONCLUSION

The objective of this work was to extend the model of binary BEC mixtures to the case when the two components are trapped by mismatched OLs. The analysis was focused on the case of the strongest mismatch, with the sublattices of opposite signs. The intrinsic nonlinearity in one species was self-attractive, while in the other one it might have either sign; however, the inter-species interaction was always attractive. Due to the opposite signs of the two effective OL potentials, the bound state of two solitons could be unstable, as the second component of this state had to

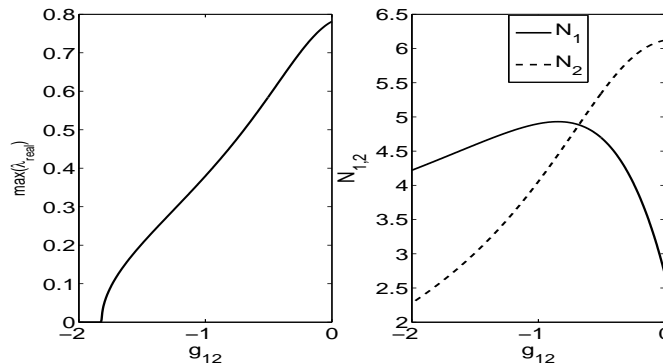


FIG. 8: (Color online) Left panel: the largest instability growth rate for solitons of the gap-bright type. Right panel: the evolution of the norms of both components with the decrease of  $g_{12}$  from 0 to  $-2$ . The parameters chosen are  $V_{01} = V_{02} = 1$ ,  $\mu_1 = 0.6$ ,  $\mu_2 = -0.3$ ,  $g_{11} = 1$ ,  $g_{22} = -1$ .

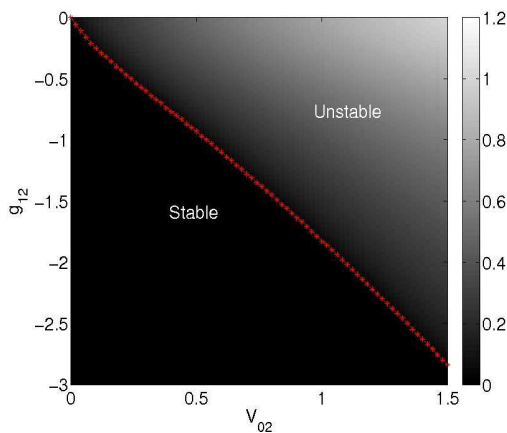


FIG. 9: (Color online) The stability diagram for solitons of the gap-bright type in the plane of  $V_{02}$  and  $g_{12}$ . The notation is the same as in Fig. 4. Other parameters are fixed:  $V_{01} = 1$ ,  $\mu_1 = 0.6$ ,  $\mu_2 = -0.3$ ,  $g_{11} = 1$ ,  $g_{22} = -1$ .

be centered around a local potential maximum. In both cases when the nonlinearity in the stable component (the one centered around the respective potential minimum) is self-attractive or self-repulsive (while the other species is self-attractive), we have identified stability regions for the soliton complexes, varying the strength of the inter-species attraction and of the OL depth. In cases when the soliton complex is unstable, direct simulations have made it possible to identify basic scenarios of the instability development, which amount to the spontaneous symmetry breaking (SSB) and resulting oscillations of one or both components. In the case of the soliton complex of the “gap-bright” (GB) type, the unstable (“bright”) component may also potentially split into two unequal parts, which oscillate around different local potential minima. It is relevant to mention that it was not possible to implement a different type of the instability, where the gap-type component (the intrinsically self-repulsive one) would be originally set in an unstable position with respect to its sublattice, as a complex of such a type could *never* be constructed (even as a formal solution). For the same reason, we did not consider complexes of the gap-gap type.

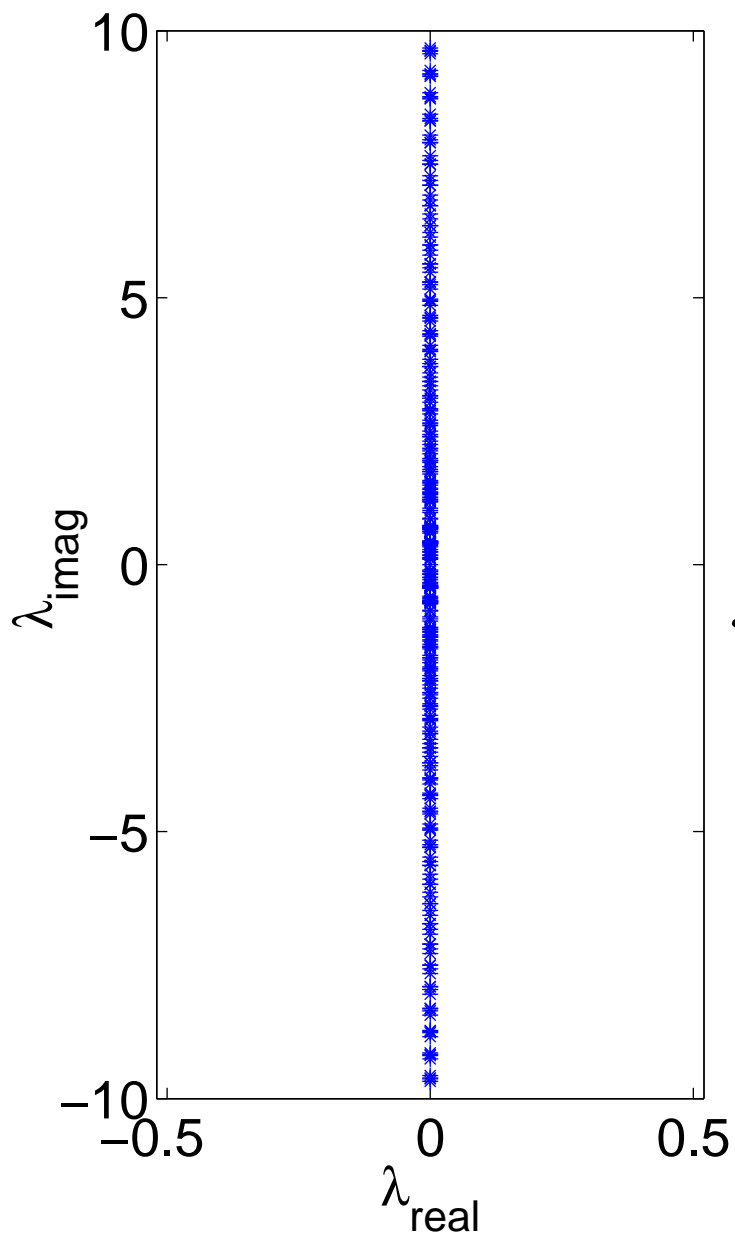
As concerns possible extensions of this work, an interesting issue is to consider the stability and dynamics of two-component solitons in two dimensions, that would be supported by two square lattices with the phase shift of  $\pi$  in both directions  $x$  and  $y$ . In that case, it would be interesting to examine whether the unstable component may perform two-dimensional quasi-circular motion around the pinned stable one.

[1] O. Morsch and M. Oberthaler, Rev. Mod. Phys. **78**, 179 (2006).

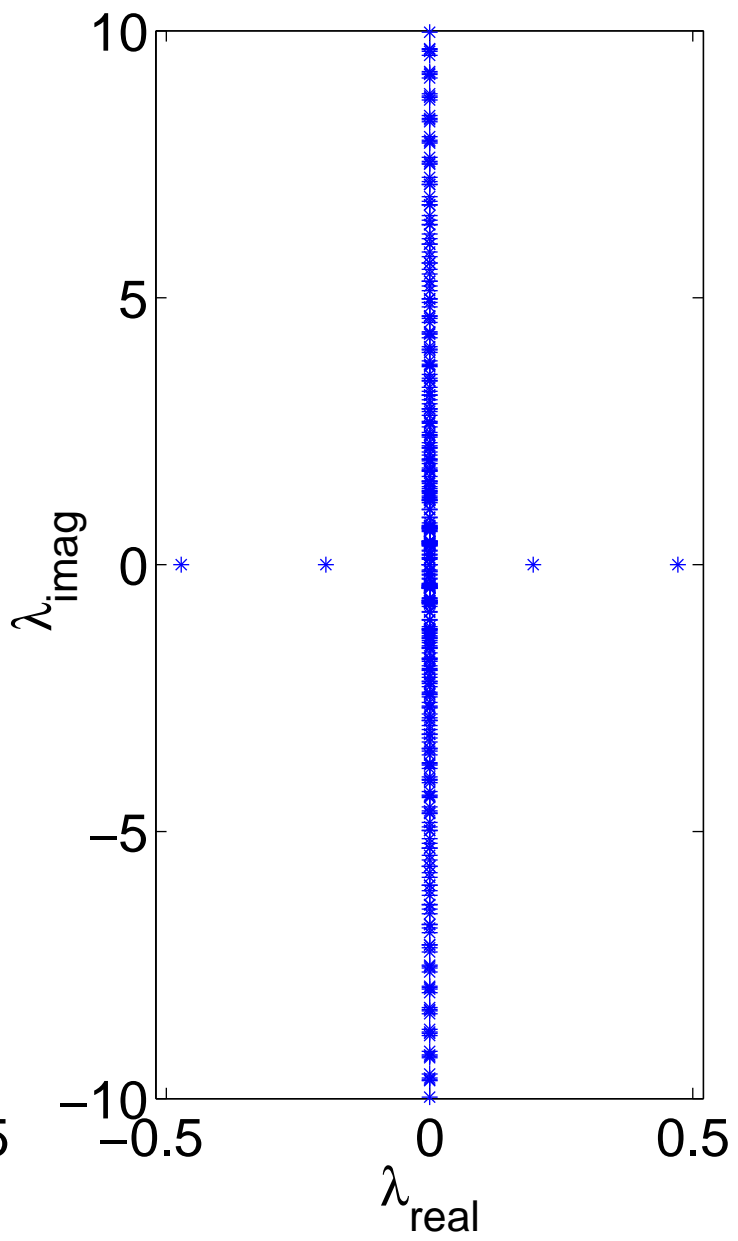
[2] F. Kh. Abdullaev, B. B. Baizakov, S. A. Darmanyan, V. V. Konotop, and M. Salerno, Phys. Rev. A **64**, 043606 (2001); I.

- Carusotto, D. Embriaco, and G. C. La Rocca, *ibid.* **65**, 053611 (2002); B. B. Baizakov, V. V. Konotop and M. Salerno, J. Phys. B **35**, 5105 (2002); E. A. Ostrovskaya and Y. S. Kivshar, Phys. Rev. Lett. **90**, 160407 (2003).
- [3] B. Eiermann, Th. Anker, M. Albiez, M. Taglieber, P. Treutlein, K.-P. Marzlin, and M. K. Oberthaler, Phys. Rev. Lett. **92**, 230401 (2004).
- [4] B. A. Malomed, Z. H. Wang, P. L. Chu, and G. D. Peng, J. Opt. Soc. Am. B **16**, 1197 (1999).
- [5] G. L. Alfimov, V. V. Konotop, and M. Salerno, Europhys. Lett. **58**, 7 (2002); V. A. Brazhnyi and V. V. Konotop, Mod. Phys. Lett. B **18**, 627 (2004).
- [6] C. J. Myatt, E. A. Burt, R. W. Ghrist, E. A. Cornell, and C. E. Wieman, Phys. Rev. Lett. **78**, 586 (1997); D. M. Stamper-Kurn, M. R. Andrews, A. P. Chikkatur, S. Inouye, H.-J. Miesner, J. Stenger, and W. Ketterle, Phys. Rev. Lett. **80**, 2027 (1998); D. S. Hall, M. R. Matthews, J. R. Ensher, C. E. Wieman, and E. A. Cornell, Phys. Rev. Lett. **81**, 1539 (1998).
- [7] S. Inouye, M. R. Andrews, J. Stenger, H. J. Miesner, D. M. Stamper-Kurn, and W. Ketterle, Nature **392**, 151 (1998); E. A. Donley, N. R. Claussen, S. L. Cornish, J. L. Roberts, E. A. Cornell, and C. E. Wieman, *ibid.* **412**, 295 (2001).
- [8] A. Simoni, F. Ferlaino, G. Roati, G. Modugno, and M. Inguscio, Phys. Rev. Lett. **90**, 163202 (2003).
- [9] V. M. Pérez-García and J. Belmonte-Beitia, Phys. Rev. A **72**, 033620 (2005); S. K. Adhikari, Phys. Lett. A **346**, 179 (2005); Phys. Rev. A **72**, 053608 (2005); J. Phys. A **40**, 2673 (2007).
- [10] A. Gubeskys, B. A. Malomed, and I. M. Merhasin, Phys. Rev. A **73**, 023607 (2006).
- [11] S. K. Adhikari and B. A. Malomed, Phys. Rev. A, in press.
- [12] M. Matuszewski, B. A. Malomed, and M. Trippenbach, Phys. Rev. A **76**, 043826 (2007).
- [13] A. Gubeskys and B. A. Malomed, Phys. Rev. A **75**, 063602 (2007); *ibid.* **76**, 043623 (2007).
- [14] Y. J. Tsofe and B. A. Malomed, Phys. Rev. E **75**, 056603 (2007).
- [15] A. A. Sukhorukov and Y. S. Kivshar, Phys. Rev. Lett. **97**, 233901 (2006).
- [16] N. A. Kostov, V. Z. Enol'skii, V. S. Gerdjikov, V. V. Konotop, and M. Salerno, Phys. Rev. E **70**, 056617 (2004); Y. S. Cheng, R. Z. Gong, and H. Li, Opt. Exp. **14**, 3594 (2006); H. A. Cruz, V. A. Brazhnyi, V. V. Konotop, G. L. Alfimov, and M. Salerno, Phys. Rev. A **76**, 013603 (2007).
- [17] E. A. Ostrovskaya and Y. S. Kivshar, Phys. Rev. Lett. **92**, 180405 (2004).
- [18] F. Dalfovo, S. Giorgini, L. P. Pitaevskii, and S. Stringari, Rev. Mod. Phys. **71**, 463 (1999).
- [19] T. Kapitula, Physica D **156**, 186 (2001).
- [20] S. Adhikari and B. A. Malomed, Europhys. Lett. **79**, 50003 (2007); Phys. Rev. A **76**, 043626 (2007).

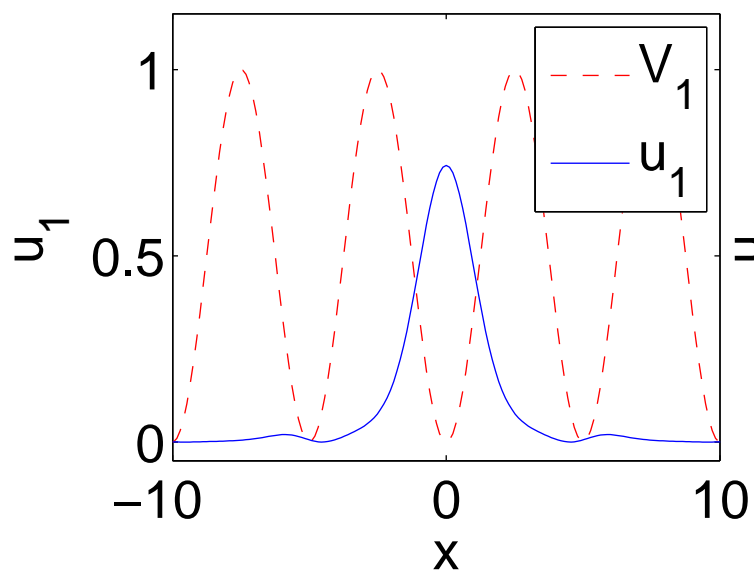
Stable



Unstable



Stable



Unstable

